J Fluoresc (2012) 22:1513–1519
DOI 10.1007/s10895-012-1089-2

ORIGINAL PAPER

A Comparative Study on the Sensitive Detection of Hydroxyl Radical Using Thiol-capped CdTe and CdTe/ZnS Quantum Dots

Oluwasesan Adegoke · Tebello Nyokong

Received: 20 March 2012 / Accepted: 20 June 2012 / Published online: 28 June 2012

Abstract Four types of water-soluble luminescent quantum dots (QDs) whose surface was functionlaized with thioglycolic acid (TGA), 3-mercaptopropionic acid (MPA), or glutathione (GSH), were investigated for the sensitive and selective detection of hydroxyl radical ($^{\bullet}$OH) in aqueous media. It was found that the type of capping agent and QD influenced the sensitivity of the probe. The order of sensitivity of the probe was: GSH-CdTe@ZnS > MPA-CdTe@ZnS > TGA-CdTe > MPA-CdTe QDs. Under the optimum conditions, a limit of detection as low as 8.5×10^{-8} M was obtained using GSH-CdTe@ZnS. The effects of foreign reactive oxygen species and the Fenton reactants and products as possible interferences on the proposed probe were negligible for CdTe@ZnS QDs. Besides, experimental results indicated that CdTe@ZnS QDs were more attractive for the selective recognition of $^{\bullet}$OH than CdTe QDs. The mechanistic reaction pathway between the QDs and $^{\bullet}$OH is proposed.

Keywords Hydroxyl radical · Quantum dots · Mercaptopropionic acid · Thioglycolic acid · Glutathione

Introduction

Reactive oxygen species (ROS) such as peroxynitrite anion ($ONOO^-$), hydrogen peroxide (H_2O_2) and hydroxyl radical ($^{\bullet}$OH) are primarily known as by-products of normal metabolism and have been extensively studied within the biological, medical and chemical fields [1–6]. $^{\bullet}$OH plays an important role in biosystems due to its strong oxidative power and high reactivity and it is thought to induce lipid peroxidation and DNA damages which are related to various diseases such as ageing [7, 8].

Several techniques such as electron spin resonance (ESR) [9], chemiluminescence [10] and oxygen consumption [11] have been employed to detect $^{\bullet}$OH. However, due to the ability of $^{\bullet}$OH to react with other products [12], these methods are not very sensitive and suitable enough to acquire quantitative information on $^{\bullet}$OH. A number of fluorescence measurements using organic fluorescent probes have also been employed for the detection of $^{\bullet}$OH [7, 13], due to high sensitivity over other techniques. Some commonly known fluorescence probes for the detection of $^{\bullet}$OH are: dichlorofluorescin (DCFH) [14], 3′-(p-aminophenyl) fluorescein (APF) [15] and 3′-(p-hydroxyphenyl) fluorescein (HPF) [16]. The most widely used fluorescence probes may react with a range of ROS if a general measurement of oxidative stress is required, but they lack specificity if an individual ROS is sought [17]. Due to this limitation, we have developed an assay for the detection of hydroxyl radical in aqueous solution using quantum dots (QDs) as fluorophore probe.

The use of QDs for the development of sensors has proven to be one of the fastest growing fields of nanotechnology due to their high fluorescence quantum yields (Φ_F), narrow emission and broad absorption spectra [18, 19]. To date, several sensors have been developed using QDs [20–24]. However, the utilization of QDs using fluorescence technique as a sensitive and selective probe for the detection of ROS has been less explored. For example, Wu and co-workers have reported the use of QDs in the discrimination of Fe^{2+} and Fe^{3+} by generating $^{\bullet}$OH via the Fenton hybrid system [25], while a chemiluminescence system based on QDs and sensitive to $^{\bullet}$OH have been reported [26, 27]. However, the lack of information on the detection limits and selectivity for $^{\bullet}$OH is

O. Adegoke · T. Nyokong (✉)
Department of Chemistry, Rhodes University,
Grahamstown 6140, South Africa
e-mail: t.nyokong@ru.ac.za

the major drawback for the published QD-based probe. Therefore, it is important to develop a suitable QDs-based probe for $^{\bullet}OH$ with unique sensitivity and selectivity by studying the interaction between different surface functionality of QDs with $^{\bullet}OH$.

Thus, it is expected that surface modification of QDs with organic ligands and the coating of the core with a higher bandgap material such as ZnS can be an effective tool for influencing their chemical, optical and photocatalytic properties which can lead to an improvement of the photostability of QDs, enhancement of their sensitivity and selectivity. In this paper, we have developed a sensor for $^{\bullet}OH$ and investigated the effect of different thiol-cappings of CdTe and CdTe@ZnS QDs on the sensitivity and selectivity of the proposed probe for the first time. The combination of steady-state and time resolved fluorescent measurements were used to unravel the interaction between QDs and $^{\bullet}OH$.

Experimental

Materials

Reduced L-glutathione (GSH), thioglycolic acid (TGA), 3-mercaptopropionic acid (MPA), $CdCl_2.2.5.H_2O$, tellurium shots, H_2O_2, t-butyl hydroperoxide (TBHP) and sodium borohydride were obtained from Sigma-Aldrich. Methanol, ethanol, $ZnCl_2$, Na_2S, $FeCl_3$, $(NH)_2Fe(SO)_2.6H_2O$, ethylenediaminetetraacetic acid (EDTA), L-ascorbic acid and tris (hydroxyl methyl) amino methane were obtained from SAARCHEM. $NaClO_4.H_2O$ was obtained from BDH chemicals. All chemicals were of analytical grade and used without prior purification. All solutions were prepared with ultra pure water obtained from a Milli-Q Water System (Millipore Corp. Bedford, MA, USA). Tris-HCl buffer (50 mM) was employed for all studies and the pH was adjusted by addition of 1.0 M NaOH or HCl. The synthesis of TGA-CdTe, MPA-CdTe, MPA-CdTe@ZnS and GSH-CdTe@ZnS QDs were as reported in literature [28–32].

Instrumentation

Excitation and emission spectra were recorded on a Varian Eclipse spectrofluorimeter. The excitation wavelength (400 nm) and slit widths (5 nm) were kept constant for all the experiments. Ground state electronic absorption spectra were recorded on a Shimadzu ultra-violet visible (UV/vis) 2550 spectrophotometer. X-ray powder diffraction (XRD) patterns were recorded using a Cu kα radiation (λ=1.5405 Å, nickel filter), on a Bruker D8 Discover equipped with a proportional counter. Scanning was at 1° min^{-1} with a filter time-constant of 2.5 s per step and a slit width of 6.0 nm, while data were obtained in the range from 2θ=5° to 60°. A zero background silicon wafer slide was used for sample placement. XRD data analysis was carried out using Eva (evaluation curve fitting) software. Subtraction of spline fitted to the curved background was used for baseline correction of each diffraction pattern and the full-width at half maximum values was obtained from the fitted curve. A Metrohm Swiss 827 pH meter was used for pH measurements. Fluorescence lifetime measurements were carried out using a time correlated single photon counting (TCSPC) setup (FluoTime 200, Picoquant GmbH). The excitation source was a diode laser (LDH-P-C-485 with 10 MHz repetition rate, 88 ps pulse width). Fluorescence was detected under the magic angle with a peltier cooled photomultiplier tube (PMT) (PMA-C 192-N-M, Picoquant) and integrated electronics (PicoHarp 300E, Picoquant GmbH). A monochromator with a spectral width of about 4 nm was used to select the required emission wavelength band. A scattering Ludox solution (DuPont) was used to measure the response function of the system and had a full width at half maximum (FWHM) of about 280 ps. To obtain good statistics, the ratio of stop to start pulses was kept low (below 0.05). Measurement of the entire luminescence decay curve (range 0 to 100 ns) was at the maximum of the emission peak. Data analysis was done using the program Fluofit (Picoquant GmbH). Estimation of the decay times was carried out using the support plane approach.

General Procedure for $^{\bullet}OH$ Detection

$^{\bullet}OH$ radicals were generated from Fe^{2+}-EDTA/H_2O_2/ascorbic acid Fenton hybrid system that mimics the production of $^{\bullet}OH$ for biological foot-printing of proteins [33] and were immediately added to a fluorescence cell containing colloidal solution of QDs in Tris-HCl buffer (50 mM) pH 7.4 (total volume=3 ml). The solution was stirred vigorously for few seconds and the fluorescence measurement was taken afterward.

Results and Discussion

Optical Properties of QDs

Figure 1A and B, presents typical absorption and fluorescence spectra of different thiol-capped CdTe and CdTe@ZnS QDs in 50 mM Tris-HCL, pH 7.4. The CdTe and CdTe@ZnS QDs exhibit broad absorption and well-resolved emission spectra. In this work, TGA-CdTe, MPA-CdTe@ZnS, MPA-CdTe, and GSH-CdTe@ZnS QDs with emission peaks at 549, 557, 564, and 600 nm (Fig. 1B) were

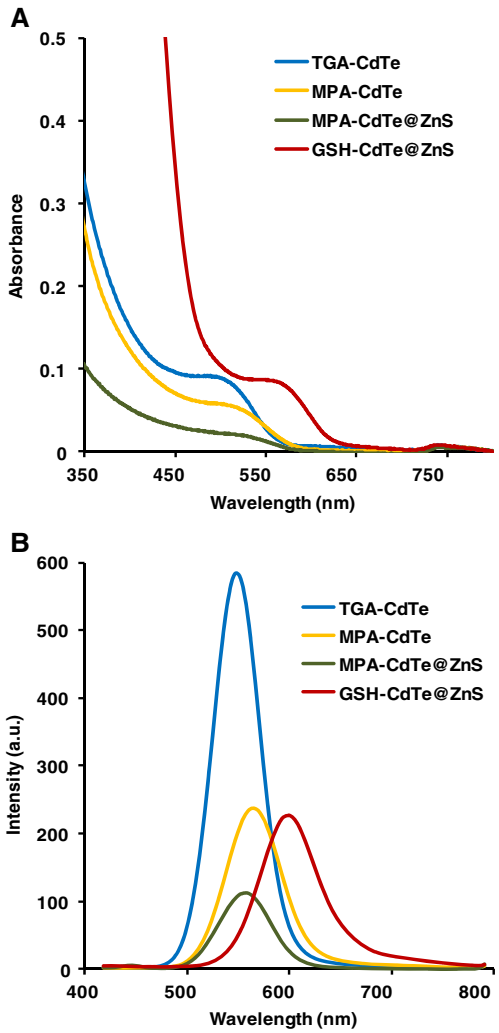

Fig. 1 UV/vis absorption (**A**) and fluorescence emission spectra (**B**) of different sized QDs. TGA-CdTe (λ_{emi}=549 nm), MPA-CdTe@ZnS (λ_{emi}=557 nm), MPA-CdTe (λ_{emi}=564 nm) and GSH-CdTe@ZnS (λ_{emi}=600 nm). Solvent: 50 mM Tris-HCL buffer, pH 7.4

employed for comparative studies as a means for developing an optimum QDs-based probe. Their corresponding fluorescence quantum yields (Φ_F) were determined according to the procedure reported in literature [34], Eq. 1:

$$\Phi_F = \Phi_{F(Std)} \frac{F \cdot A_{Std} \cdot n^2}{F_{Std} \cdot A \cdot n^2_{Std}} \quad (1)$$

where A and A_{Std} are the absorbances of the sample and standard at the excitation wavelength, respectively. F and F_{Std} are the areas under the fluorescence curves of the QDs and the standard respectively and n and n_{Std} are the refractive indices of the solvent used for the sample and standard. Rhodamine 6 G in ethanol (Φ_F=0.95 [35]) was used as the standard. The values of Φ_F were found to be 0.80, 0.47, 0.72 and 0.39 for TGA-CdTe, MPA-CdTe, MPA-CdTe@ZnS and GSH-CdTe@ZnS, respectively, Table 1.

Structural Properties of QDs

X-ray powder diffraction can provide useful information about the crystal structure and sizes of colloidal nanocrystal QDs. Figure 2 shows the X-ray diffraction patterns of TGA-CdTe and GSH-CdTe@ZnS QDs as a representation for the rest of the QDs. A typical zinc blend crystal structure [20] with planes at 111, 220, and 311 were obtained for CdTe QDs with peaks at 26.8°, 44.0° and 52.1°. The peaks for CdTe@ZnS QDs were at 28.6°, 47.6° and 56.2°. Following the growth of ZnS shell on the core CdTe, the peak position shifted to higher angles and thus confirms the formation of CdTe@ZnS coreshell QDs. The size of the QDs was determined using XRD, according to the Scherrer Eq. 2 [36].

$$d(\mathrm{A}) = \frac{k\lambda}{\beta \cos\theta} \quad (2)$$

λ is the wavelength of the X-ray source (1.5405 À), k is an empirical constant equal to 0.9, β is the full width at half maximum of the diffraction peak, and θ is the angular position. The sizes of QDs obtained from XRD calculation were TGA-CdTe (2.3 nm), MPA-CdTe (2.7 nm), GSH-CdTe@ZnS (3.0 nm) and MPA-CdTe@ZnS (3.1 nm).

Effect of pH and Buffer on the Detection Condition for $^{\bullet}$OH

GSH-CdTe@ZnS QDs was chosen as a representative for all the QDs to optimize the $^{\bullet}$OH detection conditions. Different buffers such as, phosphate buffered saline (PBS), acetate buffer, phosphate buffer, citric acid-NaOH, tris-ethylenediaminetetraacetic acid (Tris-EDTA) and Tris-HCl were examined (all at pH 7.4) and our results showed that Tris-HCL (50 mM) was best suited because it resulted in the largest quenching of the QDs fluorescence on addition of $^{\bullet}$OH. Thus Tris-HCl was selected for further experiments (Fig. 3 inset). Also, it is known that pH could have a drastic influence on the fluorescence intensity of QDs, which could affect both

Table 1 Quenching rate constant (Ksv) and limit of detection (LOD) for different QDs used for the detection of $^{\bullet}$OH. QDs sizes and fluorescence quantum yields (Φ_F) are also included. Solvent: 50 mM Tris-HCL pH 7.4

QDs	QDs size (nm)	Ksv (M^{-1})	LOD (μM)	RSD	Φ_F
TGA-CdTe	2.3	$2..0\times10^{6}$	9.7×10^{-8}	2.5	0.80
MPA-CdTe	2.7	1.5×10^{6}	2.5×10^{-7}	3.1	0.47
MPA-CdTe@ZnS	3.1	2.1×10^{6}	9.5×10^{-8}	2.3	0.72
GSH-CdTe@ZnS	3.0	2.4×10^{6}	8.5×10^{-8}	1.8	0.39

RSD = relative standard deviation

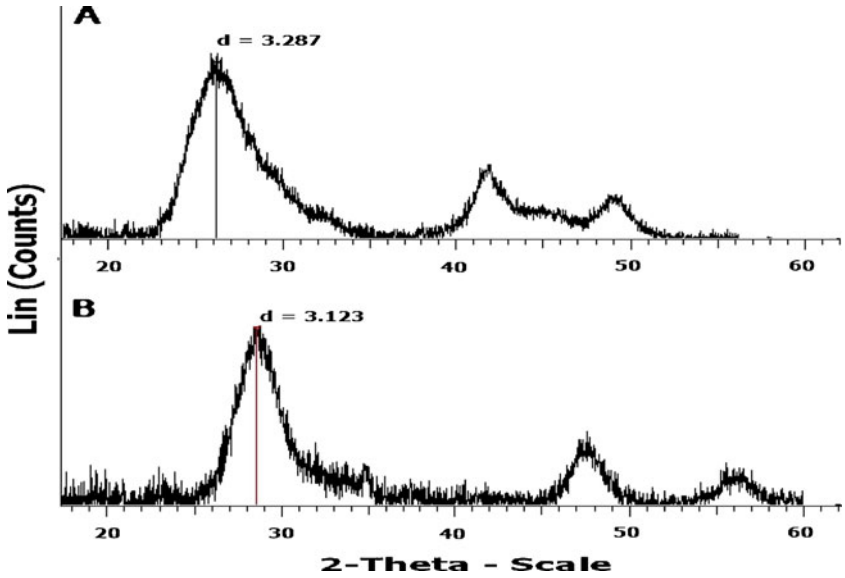

Fig. 2 Powder XRD spectra of the TGA-CdTe (**A**) and GSH-CdTe@ZnS QDs (**B**)

the sensitivity and selectivity of target analytes [18], while the capping agent is also known to be protonated at the surface of the QDs in acidic pH. As a result, the effect of pH on the fluorescence intensity of aqueous QDs-$^{\bullet}$OH system was investigated at different pH values. Figure 3 shows that there was more quenching of fluorescence of the QDs by $^{\bullet}$OH in the pH range 6.8 to 7.8. Therefore, pH 7.4, 50 mM Tris-HCL buffer was selected for further experiments.

Sensitivity of $^{\bullet}$OH on the Fluorescence Response of the QDs

Under the optimum conditions, it was found that $^{\bullet}$OH quenched the fluorescence of CdTe and CdTe@ZnS QDs

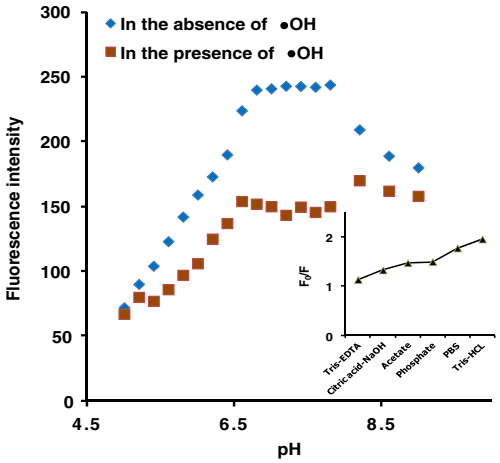

Fig. 3 Effect of pH on the fluorescence intensity of aqueous colloidal 3.0 nm GSH-CdTe@ZnS QDs in the absence and presence of $^{\bullet}$OH (C_{QDs}: 6.7×10^{-7} M, $C_{\bullet OH}$: 2.5×10^{-7} M s^{-1}, solvent: 50 mM Tris-HCl buffer). Inset: Effect of different buffers on the fluorescence intensity. F_0 and F are the fluorescence intensity of aqueous CdTe@ZnS QDs without and with $^{\bullet}$OH)

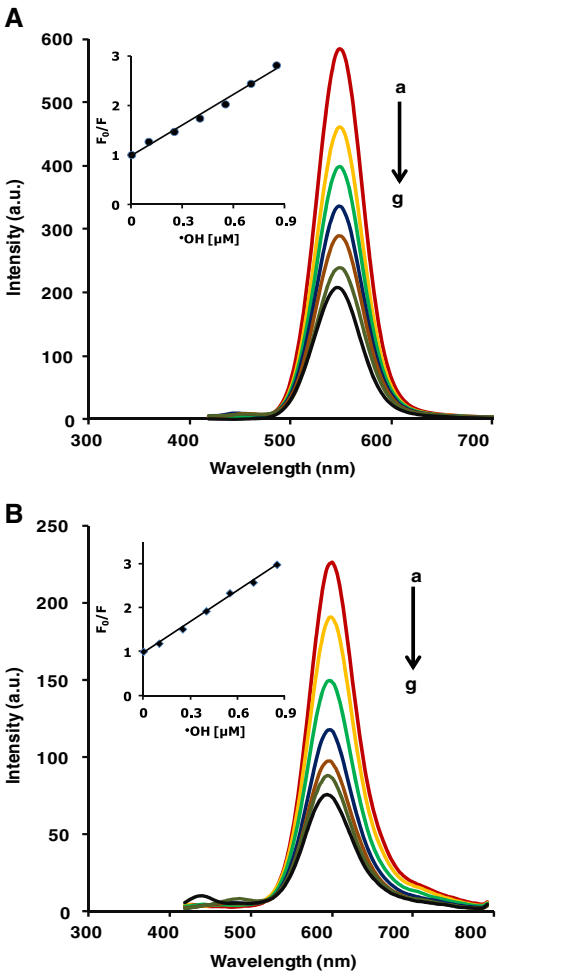

Fig. 4 Effects of addition of different concentrations of $^{\bullet}$OH on the fluorescence of 2.3 nm TGA-CdTe QDs (**A**) and 3.0 nm GSH-CdTe@ZnS QDs (**B**). ($C_{\bullet OH}$: (a) 0, (b) 1.0×10^{-7}, (c) 2.5×10^{-7}, (d) 4.0×10^{-7}, (e) 5.5×10^{-7}, (f) 7.0×10^{-7} and (g) 8.5×10^{-7} M s^{-1}. Inset: corresponding Stern-Volmer plots. Solvent: 50 mM Tris-HCL buffer pH 7.4

(Fig. 4) in a concentration-dependent manner that was best described by the linear Stern-Volmer relationship, Eq. 3:

$$\frac{F_0}{F} = 1 + K_{SV}[^{\bullet}OH] \quad (3)$$

where K_{sv} is the Stern-Volmer quenching rate constant, which is related to the quenching efficiency and was evaluated from Fig. 4 (inset). Based on the rate constant of 8×10^3 $M^{-1}s^{-1}$ [37], which has been reported for $Fe^{2+/}$EDTA Fenton's reaction, the concentration of $^{\bullet}OH$ was calculated to be 1×10^{-7}, 2.5×10^{-7}, 4.0×10^{-7}, 5.5×10^{-7}, 7.0×10^{-7} and 8.5×10^{-7} M respectively, in the presence of 4.2×10^{-7}, 1.0×10^{-6}, 1.7×10^{-6}, 2.3×10^{-6}, 2.9×10^{-6} and 3.5×10^{-6} M $Fe^{2+/}$EDTA and 3×10^{-5} M H_2O_2, according to a method described by Maki et al. [7].

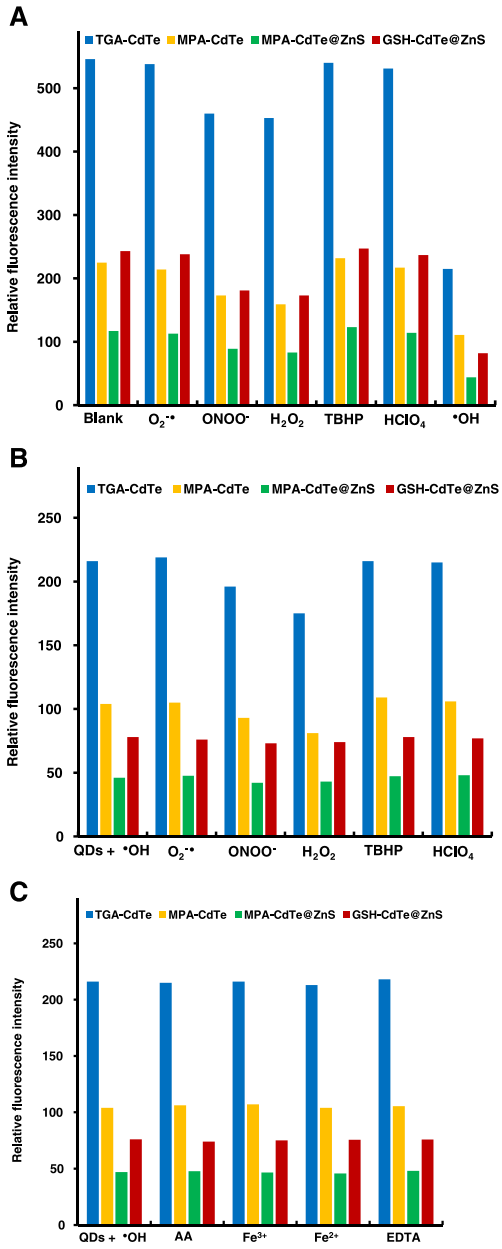

Fig. 5 **A** Effect of ROS on the fluorescence of CdTe and CdTe@ZnS QDs **B** Effect of co-existing ROS and **C** Fenton reactants and products as tested interferences on the detection of $^{\bullet}OH$ by the proposed QDs-based fluorescent probe. ($C_{O2\text{-}\bullet}$: 200 μM, $C_{ONOO\text{-}}$: 300 μM, C_{H2O2}, C_{TBHP}, C_{HCLO4}: 50 μM, C_{AA}, C_{Fe3+}, C_{Fe2+}, C_{EDTA}: 100 μM $C_{HO}{}^{\bullet}$: 0.85 μM s^{-1}). Ascorbic acid is abbreviated as AA. Solvent: 50 mM Tris-HCL buffer pH 7.4

GSH-CdTe@ZnS QDs exhibited the best sensitivity for the detection of $^{\bullet}OH$ while MPA-CdTe QDs showed the least sensitivity (comparing the K_{sv} values, Table 1). However, from our method, the coreshell CdTe@ZnS QDs were more sensitive and are best suited for the detection of $^{\bullet}OH$ than the core CdTe QDs, when comparing MPA-CdTe QDs and MPA-CdTe@ZnS QD containing the same capping agent. It was noticed that the nature of the capping agent of the QDs influenced the sensitivity of the probe (Table 1). For example, GSH capping on CdTe@ZnS has a slightly larger K_{SV} value than when MPA is employed for the same core-shell QDs even though the sizes of these QDs differ only by 0.1 nm. Also, the coating of a secondary layer with a wider bandgap semiconductor such as ZnS, passivates the surface of the QDs and can effectively enhance the non-radiative recombination pathway in the presence of a quencher leading to an increase in the quenching efficiency and stability of the nanocrsytal [38], hence MPA-CdTe@ZnS QDs show a larger K_{SV} value than MPA-CdTe QDs. The effect of thiol capping (with GSH being better than MPA for coreshell CdTe@ZnS) may be related to the reports that GSH provides better surface passivation for QDs than other thiol ligands [39]. The results suggest that the differing degree of sensitivity of the core and coreshell QDs to $^{\bullet}OH$ may depend on multiple factors. Capping agent, QD size, oxidative, photolytic and mechanical stability are individual and collective factors that can influence

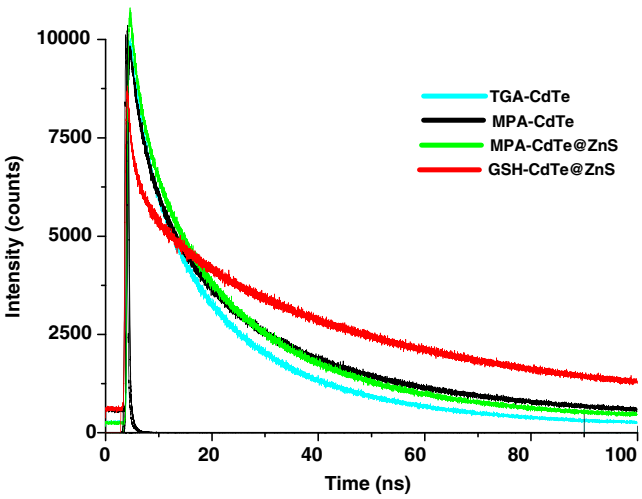

Fig. 6 Fluorescence decay curves of CdTe and CdTe@ZnS QDs in the presence of 1.0×10^{-7} M s^{-1} $^{\bullet}OH$. Solvent: 50 mM Tris-HCL pH 7.4 buffer

Table 2 Comparison of the best-fit fluorescence lifetime values for a triexponential fit of TGA-CdTe, MPA-CdTe, MPA-CdTe@ZnS and GSH-CdTe@ZnS QDs in the absence and presence of an equivalent of $^{\bullet}OH$ in 50 mM Tris-HCL buffer, pH 7.4

QDs	[$^{\bullet}OH$] (μM s^{-1})	τ_1 (ns)[a] ±0.1	τ_2 (ns)[a] ±0.07	τ_3 (ns)[a] ±0.03
TGA-CdTe	0	24.0(0.79)	7.3(0.19)	0.9(0.02)
	0.1	22.8(0.80)	7.0(0.18)	0.8(0.02)
MPA-CdTe	0	29.0(0.83)	7.0(0.15)	0.8(0.02)
	0.1	28.0(0.83)	6.4(0.15)	0.5(0.02)
MPA-CdTe@ZnS	0	33.8(0.68)	12.0(0.30)	1.4(0.02)
	0.1	31.2(0.72)	10.0(0.25)	0.9(0.03)
GSH-CdTe@ZnS	0	60.6(0.89)	16.0(0.09)	1.5(0.02)
	0.1	58.1(0.90)	13.3(0.08)	1.3(0.02)

[a]Relative abundances in brackets

the sensitivity of the QDs to $^{\bullet}OH$, hence the difference in sensitivity of core and coreshell QDs to $^{\bullet}OH$.

The limit of detection (LOD) was evaluated according to the equation LOD=3 δ/K, where δ is the standard deviation of blank measurement (n=10) and K is the slope of the calibration graph. The LOD correlated favourably with the sensitivity of the probe and the best value of 8.5×10^{-8} M was obtained for GSH-CdTe@ZnS QDs with a correlation coefficient of 0.997. The precision from six replicate measurements of 2.5×10^{-7} M $^{\bullet}OH$ was evaluated and the best reproducibility of 1.8 % was obtained for GSH-CdTe@ZnS QDs (Table 1).

Selectivity

A high selectivity for the detection of $^{\bullet}OH$ is needed for fluorescent probes. H_2O_2, $ONOO^-$ and $^{\bullet}OH$ have been reported to quench the fluorescence of QDs [25, 40, 41] As a result, we have evaluated the effect of different ROS on the fluorescence response of CdTe and CdTe@ZnS QDs and the results showed that the fluorescence of CdTe and CdTe@ZnS QDs was sensitive to $ONOO^-$ and H_2O_2 but was more significantly quenched by $^{\bullet}OH$ (Fig. 5A). A tolerable error of ±5.0 % in the relative fluorescence intensity was taken into consideration. The effect of co-existing ROS on the fluorescence of CdTe and CdTe@ZnS QDs were studied by mixing an equivalent concentration of $^{\bullet}OH$ and an excess of interfering species. As shown in Fig. 5B, the result showed there was no significant effect on the fluorescence response of CdTe@ZnS QDs for the detection of $^{\bullet}OH$. However, for TGA-CdTe and MPA-CdTe QDs, a considerable decrease in fluorescence response was observed in the presence of $ONOO^-$ and H_2O_2 indicating that $ONOO^-$ and H_2O_2 interfered with the probe for CdTe QDs. This makes the CdTe@ZnS QDs more attractive for the selective recognition of $^{\bullet}OH$ than CdTe QDs. Therefore, it clearly shows there were negligible interferences by the tested species for CdTe@ZnS QDs, and thus demonstrating that this probe has relatively high selectivity and can detect $^{\bullet}OH$. In addition, the presence of the Fenton reagents had no effect on the detection of $^{\bullet}OH$ (Fig. 5C).

Possible Reaction Mechanism

In order to elucidate the mechanism for $^{\bullet}OH$ detection, we carried out fluorescence lifetime measurements on CdTe and CdTe@ZnS QDs respectively. Deviations from linearity of Stern-Volmer plot are attributed to a combination of static and dynamic quenching. It has also been reported that fitting the lower part of the Stern-Volmer plot gives a linear relationship for the quenching of CdSe QDs by nitroxide radicals [42], which may exclude static quenching. Fluorescence lifetimes are often employed to differentiate between dynamic and static quenching. Figure 6 shows the decay curve of CdTe and CdTe@ZnS QDs in the presence of $^{\bullet}OH$. As shown in Table 2, the fluorescence lifetime evaluated from the triexponential decay curve of CdTe and CdTe@ZnS QDs decreased on addition $^{\bullet}OH$. For dynamic quenching; the fluorescence

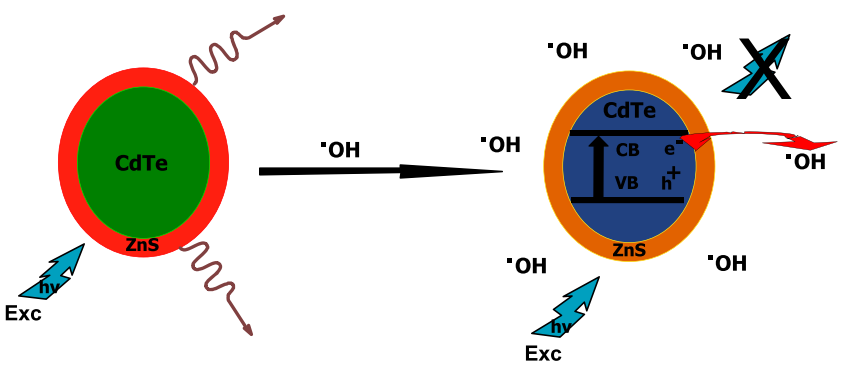

Scheme 1 The detection mechanism induced by ET from QDs to $^{\bullet}OH$

lifetimes vary with the quencher concentration while in the case of static quenching; the lifetimes are independent of quencher concentration [43]. The fact that there is a change in the lifetime with the concentration of hydroxy radical indicates that the interaction is mainly dynamic, possibly involving electron transfer (ET) processes, (Scheme 1). ET from the conduction band of GSH-capped CdTe QDs to $^{\bullet}$OH (to form hydroxyl ion) has previously been proposed [25]. We assume that since the presence of the Fenton reactants and products do not interfere with the fluorescence of QDs-HO$^{\bullet}$ probe, (as shown in Fig. 5C) then $^{\bullet}$OH is mainly responsible for the quenching of the fluorescence of CdTe and CdTe@ZnS QDs due to its strong electron accepting ability (Scheme 1).

Conclusion

A new QDs probe has been proposed for the sensitive and selective determination of $^{\bullet}$OH in aqueous media by comparative studies between different thiol-capped CdTe and CdTe@ZnS QDs. The results showed that the type of capping agent and QDs influenced the sensitivity and selectivity of the probe with GSH-CdTe@ZnS giving the best sensitivity. The mechanisms of fluorescence quenching of the QDs is mainly due to electron transfer from the conduction band of the QDs to the unoccupied band of $^{\bullet}$OH. Moreover, the proposed probe offered a LOD as low as 8.5×10^{-8} M using GSH-CdTe@ZnS QDs. Interferences from foreign ROS and the Fenton reactants and products were negligible for CdTe@ZnS QDs but CdTe QDs were not very selective towards $^{\bullet}$OH. Therefore, this system provides a new protocol for the sensitive recognition of $^{\bullet}$OH and offer additional advantages such as specificity, reproducibility, cost-effectiveness and can be adopted for the analysis of $^{\bullet}$OH in biological samples.

Acknowledgements This work was supported by the Department of Science and Technology (DST) and National Research Foundation (NRF), South Africa through DST/NRF South African Research Chairs Initiative for Professor of Medicinal Chemistry and Nanotechnology as well as Rhodes University and DST/Mintek Nanotechnology Innovation Centre (NIC) – Sensors, South Africa.

References

1. Xue Y, Luan Q, Dan Y, Yao X, Zhou K (2011) J Phys Chem C 115:4433–4438
2. Goldstein S, Samuni A (2007) J Phys Chem A 111:1066–1072
3. Goldstein S, Rabani J (2007) J Am Chem Soc 129:10597–10601
4. Samuni A, Goldstein S, Russo A, Mitchell JB, Krishna MC, Neta P (2002) J Am Chem Soc 124:8719–8724
5. Matsumoto A, Comates KE, Liu L, Stamler J (2003) Science 301:657–661
6. Melov S, Ravenscroft J, Malik S, Gill MS, Walker DW, Clayton PE, Wallace DC, Malfroy B, Doctrow SR, Lithgow GJ (2000) Science 289:1567–1579
7. Maki T, Soh N, Fukaminato T, Nakajima H, Nakano K, Imato T (2009) Anal Chim Acta 639:78–82
8. De Zwart LL, Meerman JH, Commandeur JN, Vermeulen PE (1998) Free Radical Bio Med 26:202–226
9. Wang Y, Xiong H, Zhang X, Wang S (2011) Sens Actuators B Chem 161:274–278
10. Hu Y, Zhang Z, Yang C (2008) Ultrason Sonochem 15:665–672
11. Komagoe K, Takeuchi H, Katsu T (2008) Sens Actuators B Chem 134:516–520
12. Nosaka Y, Koenuma K, Ushida K, Kira A (1996) Langmuir 12:736–738
13. Cui G, Ye Z, Chen J, Wang G, Yuan J (2011) Talanta 84:971–976
14. Bass DA, Parce JW, Dechatelet LR, Szejda P, Seeds MC, Thomas M (1983) J Immunol 130:1910–1917
15. Indo HP, Davidson M, Yen HC, Suenaga S, Tomita K, Nishii T, Higuchi M, Koga Y, Ozawa T, Majima HJ (2007) Mitochondrion 7:106–118
16. Tomizawa S, Imai H, Tsukada S, Simizu T, Honda F, Nakamura M, Nagano T, Urano Y, Matsuoka Y, Fukasaku N, Saito N (2005) Neurosci Res 53:304–313
17. Hernández-García D, Wood CD, Castro-Obregón S, Covarrubias L (2010) Free Radical Bio Med 49:130–143
18. Han B, Yuan J, Wang E (2009) Anal Chem 81:5569–5573
19. Shi L, De Paoli V, Rosenzweig N, Rosenzweig Z (2006) J Am Chem Soc 128:10378–10379
20. Dubach JM, Harjes DI, Clark HA (2007) J Am Chem Soc 129:8418–8419
21. Qian F, Zhang C, Zhang Y, He W, Gao X, Hu P, Guo Z (2009) J Am Chem Soc 131:1460–1468
22. Medintz IL, Clapp AR, Mattoussi H, Goldman ER, Fisher B, Mauro JM (2003) Nature 2:630–638
23. Freeman R, Liu X, Willner I (2011) Nano Lett 11:4456–4461
24. Ji X, Zheng J, Xu J, Rastogi VK, Cheng T, DeFrank JJ, Lablanc RM (2005) J Phys Chem B 109:3793–3799
25. Wu P, Li Y, Yan X (2009) Anal Chem 81:6252–6257
26. Chen H, Lin L, Lin Z, Guo G, Lin J (2010) J Phys Chem A 114:10049–10058
27. Jiang H, Ju H (2007) Anal Chem 79:6690–6696
28. Jiang Z, Leppert V, Kelley DF (2009) J Phys Chem C 113:19161–19171
29. Dong C, Qian H, Fang N, Ren J (2006) J Phys Chem B 110:11069–11075
30. Zhang H, Zhou Z, Yang B (2003) J Phys Chem B 107:8–13
31. Jhonsi MA, Renganathan R (2010) J Colloid Interface Sci 344:596–602
32. Liu Y, Yu J (2010) J Colloid Interface Sci 351:1–9
33. Xu G, Chance MR (2007) Chem Rev 107:3514–3543
34. Fery-Forgues S, Lavabre D (1999) J Chem Ed 76:1260–1264
35. Zhang H, Zhou Z, Yang B, Gao M (2003) J Phys Chem B 107:8–13
36. Sapra S, Sarma DD (2005) Pramana 65:565–570
37. Sutton HC, Winterbourn CC (1989) Free Radical Bio Med 6:53–60
38. Green M (2010) J Mater Chem 20:5797–5809
39. Tortiglione C, Quarta A, Tino A, Manna L, Cingolani R, Pellegrino T (2007) Bioconjugate Chem 18:829–835
40. Priyam A, Bhattacharya SC, Saha A (2009) Phys Chem Chem Phys 11:520–527
41. Gill R, Bahshi L, Freeman R, Willner I (2008) Angew Chem Int Ed 47:1676–1679
42. Gadenne B, Yildiz I, Amelia M, Ciesa F, Secchi A, Arduini A, Credi A, Raymo FM (2008) J Mater Chem 18:2022–2027
43. Wang X, Qu L, Zhang J, Peng X, Xiao M (2003) Nano Lett 3:1103–1106